Gorini, D. N. & Callisto, L. *Géotechnique* [https://doi.org/10.1680/jgeot.19.TI.012]

A macro-element approach to analyse bridge abutments accounting for the dynamic behaviour of the superstructure

DAVIDE NOÈ GORINI* and LUIGI CALLISTO†

This paper describes an original approach to the study of the seismic behaviour of bridge abutments. The proposed method incorporates a simplified description of the dynamic response of the bridge structure into a finite-element model of the soil–abutment system. Specifically, the dynamic behaviour of the bridge structure is described by a macro-element that simulates the loads transferred to the abutment during the seismic event. The macro-element is identified using a structural model of the bridge as a reference. This approach improves the current analysis methods based on sub-structuring, limiting at the same time the computational demand needed for a complete study of the soil–structure interaction. In the paper, the validity of the procedure is demonstrated comparing the results of the simplified approach with the results obtained from full three-dimensional dynamic analyses of idealised soil–bridge systems, using non-linear advanced constitutive models to describe the soil behaviour. Based on these results, a strategy is devised for the calibration of the bridge macro-element, making use of a limited number of input parameters.

KEYWORDS: design; dynamics; numerical modelling; soil/structure interaction

INTRODUCTION

Bridge abutments closely interact with the soil below their foundation and with the approach embankment. Therefore, they can be regarded as a particular case of embedded foundations for which the load transfer mechanism occurs both at their base and at the lateral surface. In a girder bridge, the abutment can be either weakly or strongly connected with the bridge deck, depending on the number of force components that may be exchanged between the two systems during a seismic event. In particular, during an earthquake a strong abutment exhibits an important interaction with the bridge structure and with both the foundation and embankment soil volumes. This is an intricate phenomenon, which in principle should be analysed with a direct approach, entailing the development of a full three-dimensional model including the entire structure of the bridge and a substantial soil volume. However, the complexity of such a direct approach and the related computational efforts make this method practically unfeasible for the design of large structures. A different way to tackle this soil–structure interaction would be to use a sub-structure approach (Kausel, 2010), in which the response of the soil–abutment system would be simulated in the structural analysis with a dynamic impedance matrix and the abutment itself would be designed applying the reaction forces derived from the structural analysis on a local model of the soil–abutment system, including in this local model the inertial actions deriving from the masses of the soil and the abutment structure (Callisto & Rampello, 2013). But this decoupled approach is made problematic by the difficulties in representing an abutment using a dynamic impedance matrix, deriving from the strong non-linearity and asymmetry of its response, and by the important inertial effects associated with the mass of soil interacting with the abutment.

An intermediate approach to this problem was adopted for instance by Callisto *et al*. (2013), which, in the seismic analysis of the Messina Strait suspension bridge, introduced a simplified description of the bridge structure in the numerical models of its embedded foundations. The methodology presented in this paper, developed explicitly for bridge abutments, is in line with the idea of including in a local model of the soil–foundation system a partial coupling with the dynamic response of the bridge structure. This is done introducing a macro-element representation of the behaviour of the structure of the bridge in the local model of the soil–abutment system. This approach was originally used by Price & Eberhard (2005), who developed a linear frequency-dependent model to simulate the contribution of the first global model of the bridge structure to the dynamic behaviour of an abutment, neglecting its potentially non-linear behaviour and the contribution of the higher vibration modes. Conversely, in the present work the macro-element description of the bridge structure aims to reproduce the generalised, multi-modal interaction with the abutment, accounting for the non-linear effects in the structure.

A MACRO-ELEMENT DESCRIPTION OF THE BRIDGE STRUCTURE

Definition and calibration

The dynamic behaviour of the bridge structure can be included in the analysis of the soil–abutment system through a macro-element that replicates the loads exchanged at the deck–abutment contact during a seismic event. The macro-element approach is depicted conceptually in Fig. 1: the full soil–bridge model of Fig. 1(a) is replaced by the local model of Fig. 1(b), in which the bridge structure is simulated by a second-order transfer tensor $\boldsymbol{K}_{ij}$. As shown schematically in Fig. 1, this transfer tensor is taken to express a frequency-dependent relationship between the vector of the generalised displacements $\boldsymbol{u}_j$ of the bases of the abutments and the piers,

Manuscript received 25 January 2019; revised manuscript accepted 14 November 2019.
Discussion on this paper is welcomed by the editor.
* Sapienza University of Rome, Rome, Italy (Orcid:0000-0001-6673-0071).
† Sapienza University of Rome, Rome, Italy (Orcid:0000-0001-9795-7420).

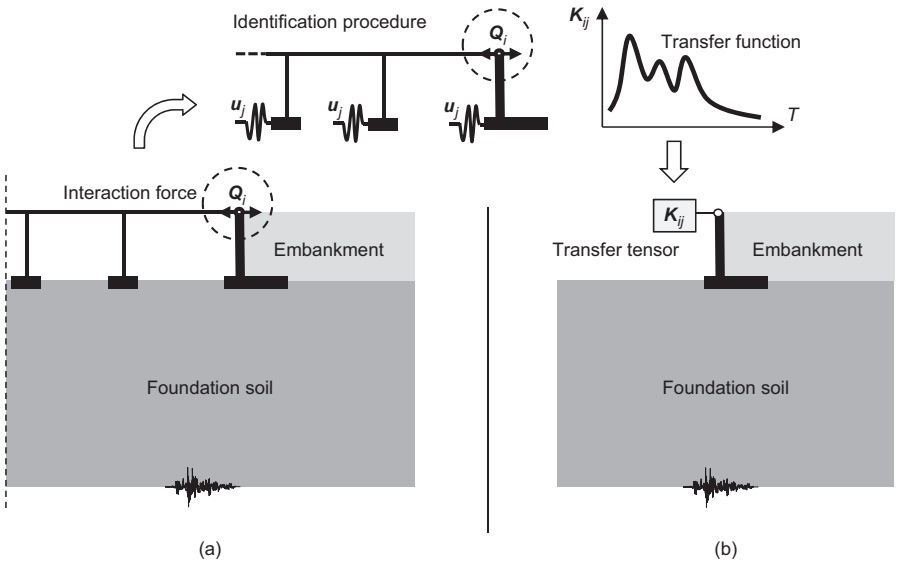

Fig. 1. Conceptual scheme of the method of the structural macro-element: (a) full soil–bridge model; (b) local model of the abutment with macro-element

and the vector of the generalised forces $\boldsymbol{Q}_i$ exchanged at the deck–abutment contact

$$\boldsymbol{Q}_i = \boldsymbol{K}_{ij} \cdot \boldsymbol{u}_j \tag{1}$$

where all the quantities depend of the vibration period T of the input motion $\boldsymbol{u}_j$. The transfer tensor can be considered an intrinsic property of the structure, not affected by the presence of the soil and depending only on the mechanical properties of the bridge: it describes the filtering effect of the bridge structure on the interaction forces exchanged by the abutment and the superstructure, taking expressly into consideration their actual connection. Each term of the tensor is a transfer function: if the dynamic response of the structure is linear, the transfer functions are independent of the amplitude of the external perturbation; conversely, when the behaviour of the bridge structure is non-linear, the transfer functions depend on the amplitude of the structural response.

For a bridge structure with a linear behaviour, the calibration of one of the transfer functions is obtained as follows: a numerical model of the structure, including the structural members and the abutments, is perturbed by a frequency sweep applied at the base of the piers and at the abutment foundations; for each vibration frequency, the maximum value of the interaction forces produced at the deck–abutment contact is determined; the transfer function is then evaluated at each frequency as the ratio of the interaction force to the amplitude of the input motion. In general, multi-modal transfer functions are obtained. These are reproduced in a local numerical model of the soil–abutment system (Fig. 1(b)) through an assembly of simple rheological systems, including the appropriate masses that confer a frequency-dependent response to the macro-element.

The appropriateness of linear macro-elements obtained with this procedure was tested for a simple, idealised soil–bridge system, in which both the structure and the soil are regarded as linear elastic materials. Consider the finite-element model depicted in Fig. 2, including a simple portal in contact with the soil through the pier foundation and an abutment with shallow foundations. The analysis of this system was performed using the analysis framework OpenSees (McKenna, 1997; McKenna *et al*., 2000) while the software GID (Diaz & Amat, 1999) was employed to generate the mesh. This simple model was conceived as a plane-strain scheme for the soil, and a plane-stress scheme for the bridge structure. The model was built with a three-dimensional mesh, with a unit length in the out-of-plane direction: the soil, the abutment and the pier foundation deform in plane strain while the bridge structure is described in its actual three-dimensional geometry, and only the longitudinal and vertical components of the seismic motion are considered.

The bridge structure consists of a deck connected by a hinge to the abutment and by a rigid constraint to the pier. This simple configuration may represent the longitudinal bridge–abutment interaction for the case of a girder bridge with a discontinuous deck. The abutment has a very similar geometry as the case study of the Pantano viaduct (Gorini & Callisto, 2017): it consists of a 13·5 m high wall, with a thickness of 4 m, resting on a shallow foundation with a length and thickness of 17·5 m and 5 m, respectively. A visco-elastic behaviour was assigned to the structural elements, with an elastic modulus relative to a C32/40 strength class concrete in European standards. In order to focus on the response of the macro-element, the entire soil domain was assumed to be dry. The foundation soil consists of a uniform layer starting from the structure foundations down to a depth of 88 m, where the ground motion is applied as a displacement–time history. The foundation soil is characterised by a shear wave velocity $V_S = 205$ m/s, while values of V_S of 228 m/s and of 434 m/s were assumed for the embankment and the backfill, respectively, reflecting values prescribed by the technical provisions for the Pantano viaduct. The soil elements were provided with a proportional (Rayleigh) viscous damping calibrated with the corner frequencies of 0·05 Hz and 15 Hz at $\xi = 2\%$ in order to produce a damping ratio of about 0·5% at the fundamental period of the soil deposit ($T_0 \approx 1{\cdot}7$ s), representing energy dissipation at small strains.

Since there is no transmission of moments at the deck–abutment contact, the behaviour of the bridge structure can be described by a two-dimensional macro-element as follows

$$\begin{bmatrix} \boldsymbol{Q}_1 \\ \boldsymbol{Q}_3 \end{bmatrix} = \begin{bmatrix} \boldsymbol{K}_{11} & \boldsymbol{K}_{13} \\ \boldsymbol{K}_{31} & \boldsymbol{K}_{33} \end{bmatrix} \begin{bmatrix} \boldsymbol{u}_1 \\ \boldsymbol{u}_3 \end{bmatrix} = \begin{bmatrix} \boldsymbol{K}_{11} & 0 \\ 0 & \boldsymbol{K}_{33} \end{bmatrix} \begin{bmatrix} \boldsymbol{u}_1 \\ \boldsymbol{u}_3 \end{bmatrix} \tag{2}$$

where the suffixes 1 and 3 denote the longitudinal and the vertical directions, respectively. The coupling terms $\boldsymbol{K}_{13}$ and $\boldsymbol{K}_{31}$ were set equal to zero, neglecting for simplicity the directional coupling of the structural response, but in

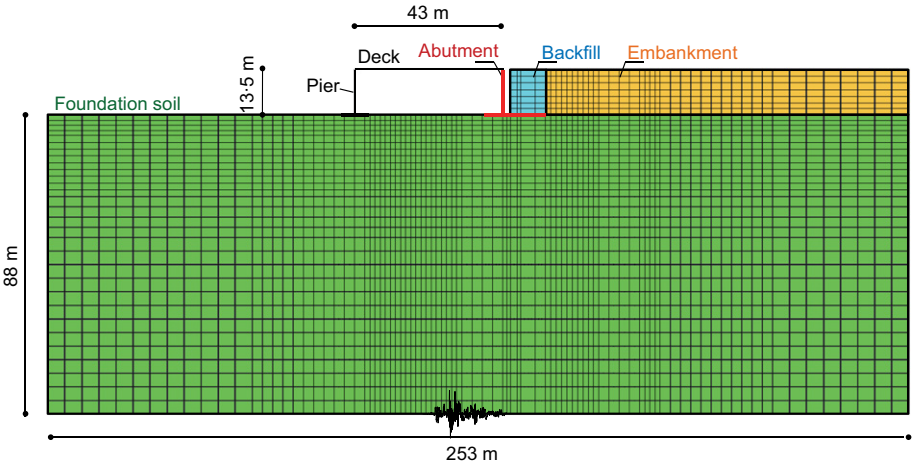

Fig. 2. Finite-element mesh of a mixed plane-strain interaction model

principle there are no difficulties in the calibration of these terms, retrieving the force Q_3 induced by the displacement field u_1 applied at the foundation level to evaluate $\boldsymbol{K}_{31}$, and vice versa for $\boldsymbol{K}_{13}$.

The longitudinal transfer function $\boldsymbol{K}_{11}$ of the structure, depicted in Fig. 3 with a continuous line, shows a maximum at high frequencies, because the interaction force $\boldsymbol{Q}_1$ is mainly governed by the dynamic axial response of the deck, that is activated by the second vibration mode of the abutment wall occurring at a period $T = 0{\cdot}01$ s. A second minor peak, occurring at $T \approx 0{\cdot}2$ s, is related to the first global mode of the structure involving the deformation of both the vertical elements but not the dynamic response of the deck: this would be the reference peak in the calibration of the equivalent single-degree-of-freedom (SDOF) system proposed by Price & Eberhard (2005). However, since this second peak has a low amplitude, the longitudinal transfer function $\boldsymbol{K}_{11}$ can be approximated by a mono-modal curve. Specifically, this response was modelled as a SDOF system, calibrating its mass $m^{(1)}$, stiffness $k^{(1)}$ and damping $\xi^{(1)}$ to produce, when combined with the dynamic response of the abutment, a reasonable approximation of the transfer function of the structure, as shown by the corresponding dotted line in Fig. 3. As a result of a trial-and-error procedure, the optimum mass and stiffness of the macro-element are $m^{(1)} = 0{\cdot}15 \times m^{(\mathrm{deck})}$ and $k^{(1)} = 3{\cdot}9 \times k^{(\mathrm{deck})}$, in

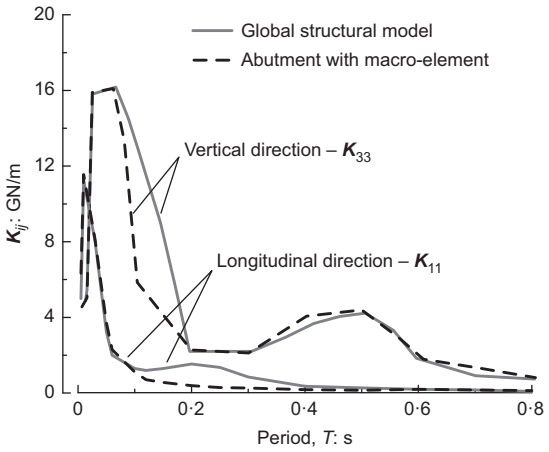

Fig. 3. Transfer functions in the longitudinal and vertical directions: comparison between the response of the entire structure and the model of abutment with macro-element

which $m^{(\mathrm{deck})}$ and $k^{(\mathrm{deck})}$ are the mass and the axial stiffness of the deck, respectively. A damping ratio $\xi = 2\%$ was assigned to the macro-element, equal to that assumed for the bridge structure in the full model of Fig. 2. By comparing the results of this identification procedure with the modal information of the structure, it was found that the mass $m^{(1)}$ of the macro-element is equal to the mass of the deck that participates in the second mode of the vertical elements. On the contrary, the stiffness $k^{(1)}$ that makes the maximum amplification occur at $T = 0{\cdot}01$ s is much larger than the axial stiffness of the deck, indicating that the characteristics of the macro-element differ considerably from the static properties of the deck.

The vertical response, represented by the transfer function in Fig. 3, shows a more pronounced bimodal trend, with a dominant peak at $T = 0{\cdot}07$ s and a second peak at $T = 0{\cdot}5$ s. The former period is associated with a global mode in which the second vertical mode of the deck combines with the vertical modes of the abutment and the pier, leading to a very stiff response and to a high value in the transfer function $\boldsymbol{K}_{33}$. The second peak is associated with the first vertical mode of the deck alone, not involving the vertical elements, leading to a longer response with a much lower value of $\boldsymbol{K}_{33}$. This vertical transfer function can be modelled with a two-degrees-of-freedom (2DOF) system. The modal mass and damping associated with the peaks of the transfer function were used to calibrate the macro-element: the first SDOF was aimed at reproducing the dominant response of the structural system (peak at $T = 0{\cdot}07$ s) and has a mass equal to $0{\cdot}6 \times m^{(\mathrm{deck})}$; this is connected in series to another SDOF with a second mass equal to $0{\cdot}9 \times m^{(\mathrm{deck})}$, representing the first participating mass of the deck in the vertical direction (peak at $T = 0{\cdot}5$ s). The stiffness was defined through a trial-and-error procedure.

Validation

A local finite-element model of the abutment, including the embankment and the foundation soil (Fig. 1(b)) was developed as a sub-set of the model in Fig. 2, including the macro-elements representation of the bridge structure resulting from the above identification procedure. For both the complete model in Fig. 2 and the local model, time-domain dynamic analyses were carried out by applying the longitudinal and the vertical components of the Tabas record (record references: NGA_143TABAS in the PEER Ground Motion Database, Section NGA-West2 (PEER Center, 2019)) to the base of the respective finite-element models.

Fig. 4(a) shows the acceleration–time histories of this seismic record and Fig. 4(b) plots the corresponding 5%-damped elastic response spectra.

Figure 5 shows a comparison between the response at the deck–abutment contact computed with the full model and with the local model that included the macro-element. Specifically, Figs 5(a) and 5(b) show the time histories of the forces $\boldsymbol{Q}_1$ and $\boldsymbol{Q}_3$ exchanged at the deck–abutment connection (note the different scales of the Q axes, reflecting the different values of the respective transfer functions). Figs 5(c) and 5(d) plot the 5%-damped elastic response spectra of the motion computed at the abutment top along both the longitudinal and the vertical directions. It is evident that the macro-element is able to reproduce with reasonable accuracy the interaction forces and the motion at the top of the abutment in both directions. Therefore, the analysis of this simple linear case shows that the macro-element of the bridge structure presented in this work can be used to reproduce the dynamic behaviour of the bridge structure in a local numerical model of the soil–abutment system.

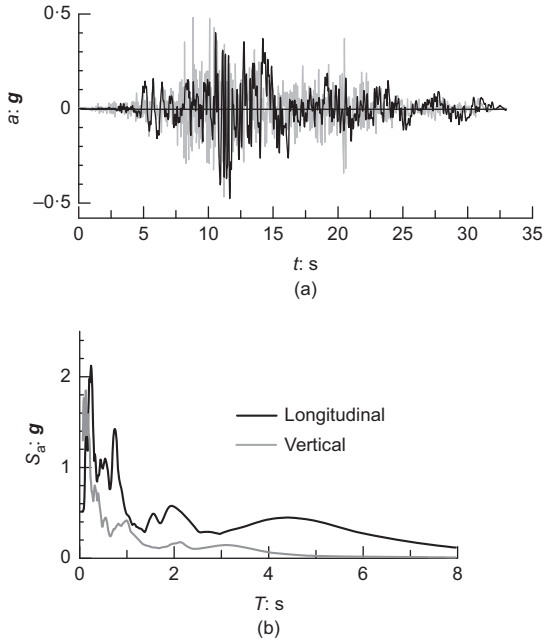

Fig. 4. (a) Time histories and (b) 5%-damped elastic response spectra of the Tabas record

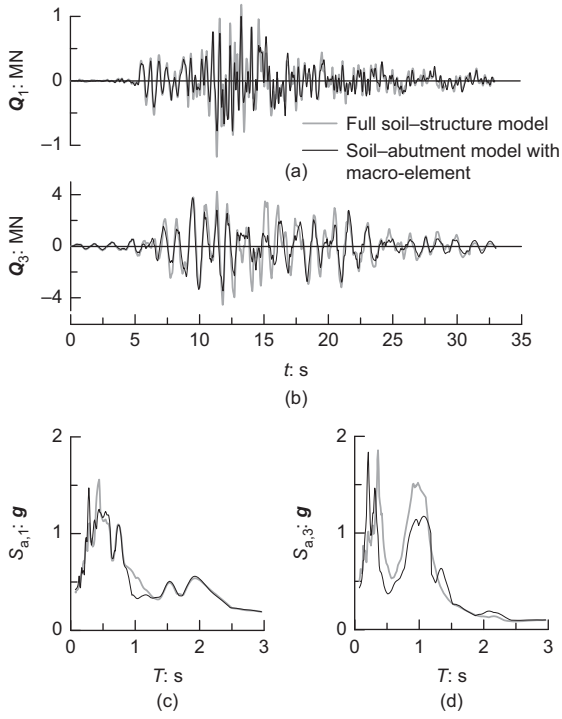

Fig. 5. Comparison between the seismic actions exchanged at the deck–abutment contact obtained with the full soil–structure model and with the local model of the soil–abutment system with macro-element: (a), (b) time histories of the longitudinal and vertical interaction forces; (c), (d) 5%-damped elastic response spectra at the abutment top

Effects of non-linearity

Under severe ground shaking, the structural response can no longer be regarded as linear. To account for this effect, a non-linear force–displacement relationship can be introduced into the macro-element formulation to make the terms of the transfer tensor dependent on the motion amplitude.

To appreciate the importance of non-linearity, the full model of Fig. 2 was modified modelling the bridge structure with the three-dimensional fibre-section force-based beam–column elements available in the OpenSees library (Neuenhofer & Filippou, 1997, 1998) in which each fibre of the structural section has an elastic–perfectly plastic behaviour. A discretisation of about one fibre every 0·1 m was adopted for the cross-section of the structural members on the basis of a sensitivity analysis. A unique yield force was considered for all the fibres, equal to 10 MN, giving a different global strength for each of the structural sections of the abutment, the deck and the pier.

This same non-linear structural model was used to identify the non-linear macro-element, carrying out on this structural system an incremental dynamic analysis (Vamvatsikos & Cornell, 2002): the structure was perturbed with harmonic longitudinal displacements of different amplitudes, applied to the abutment and the pier foundations with periods varying between 0·005 s and 1·0 s. The minimum amplitude $\boldsymbol{u}_{1,\mathrm{el}}$ of the input motion was equal to 0·01 m, corresponding to a linear response of the structure. Conversely, the maximum amplitude of the input motion $\boldsymbol{u}_{1,\max}$ was selected as the amplitude that activates a plastic mechanism in the structure. The transfer functions obtained in this identification procedure depend on the input displacement amplitude $\boldsymbol{u}_1$. Fig. 6 depicts these transfer functions as a relationship between the period T of the input motion, the amplitude $\boldsymbol{u}_1$, and the corresponding force amplitude at the deck–abutment connection $\boldsymbol{Q}_1$. The maximum value of $\boldsymbol{Q}_1$, found at $T = 0{\cdot}01$ s, increases rapidly with $\boldsymbol{u}_1$, up to a value of about $\boldsymbol{Q}_{1,\mathrm{ult}} = 1{\cdot}7$ GN, that represents a limiting value for the interaction force $\boldsymbol{Q}_1$. The values of $\boldsymbol{Q}_1$ for any other period are seen to tend asymptotically to the same value of $\boldsymbol{Q}_{1,\mathrm{ult}}$, that is therefore independent of T: the quantity $\boldsymbol{Q}_{1,\mathrm{ult}}$ is related only to the ultimate resistance of the structure and not to its dynamic response.

If the values of the interaction force $\boldsymbol{Q}_1$ shown in Fig. 6 are plotted as a function of the amplitude $\boldsymbol{u}_1$ of the input motion, for the four most significant periods of 0·005 s, 0·01 s, 0·05 s and 0·2 s, one can obtain the desired non-linear relationship that describes the transfer functions. In Fig. 7 this relationship is shown in a non-dimensional form, where the interaction force is divided by $\boldsymbol{Q}_{1,\mathrm{ult}}$ and the input displacement is divided by $\boldsymbol{u}_{1,\mathrm{ult}}$, which is the input amplitude associated with the attainment of $\boldsymbol{Q}_{1,\mathrm{ult}}$. This normalised relationship between force and displacement amplitudes could be approximated with a unique hyperbolic curve, as

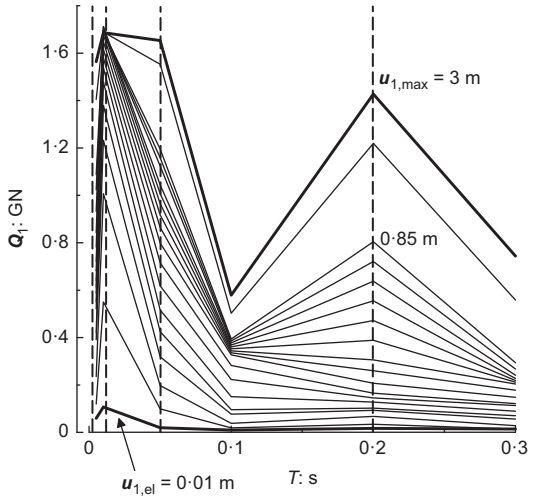

Fig. 6. Longitudinal force at the abutment top obtained for different amplitudes u_1 of the input motion: from a purely elastic structural response ($u_1 = u_{1,el}$) to a diffused plastic response (asymptotic value $Q_1 = Q_{1,ult}$)

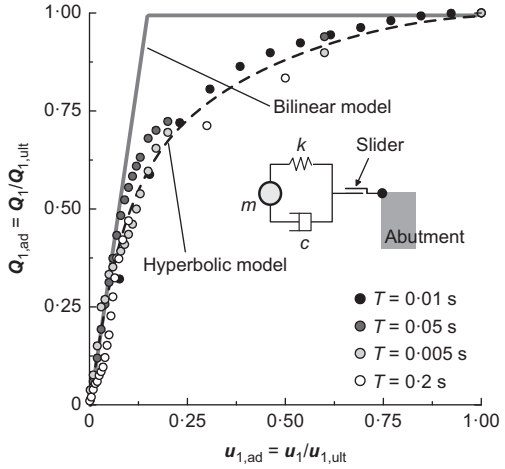

Fig. 7. Normalised maximum interaction force $Q_{1,ad}$ plotted as a function of the intensity factor $u_{1,ad}$ of the input motion: non-linear force–displacement relationships of the macro-element of the bridge structure

shown in the figure. Because it is convenient to describe this non-linear effect with a simple assembly of rheological elements, the normalised representation was approximated by the bilinear relationship shown in Fig. 7. This allows the non-linearity of the bridge structure to be modelled combining the elastic transfer tensor with a perfectly plastic element (fuse) calibrated to reproduce the ultimate capacity of the structural system, for each degree of freedom of the deck–abutment contact. This solution can be particularly representative of cases in which the structural non-linearity derives from deck isolating devices.

As for the linear case, the bilinear macro-element of the bridge structure obtained with the above procedure was used within a local model of the soil–abutment system to reproduce the behaviour resulting from a dynamic analysis of the full model in Fig. 2, in which both the soil and the structure exhibit non-linear behaviour. In these analyses, the non-linear behaviour of the soil was described using the elastic–plastic pressure-dependent multi-yield (PDMY) constitutive model proposed by Yang *et al*. (2003), calibrated in order to have the same initial tangent stiffness as the visco-elastic material used in the linear analyses. The PDMY is a multi-surface plasticity model with kinematic hardening in which, after the first yield, the stiffness decreases progressively until an ultimate surface in the stress space is reached. The set of parameters of the PDMY model used for the soil domain are reported in Table 1. The analyses were carried out in terms of effective stresses, assuming a drained condition due to the absence of pore water.

For the sake of conciseness, the validation presented herein refers to the sole longitudinal component of the Tabas record. The results obtained with the full soil–structure model and with the local soil–abutment model employing the non-linear macro-element are compared in Fig. 8. The response spectra of Fig. 8(b) show that the non-linear macro-element captures quite closely the seismic motion transmitted by the bridge deck to the top of the abutment. The corresponding forces $\boldsymbol{Q}_1$, shown in the time history of Fig. 8(a), are reproduced well during strong motion, in both their time variation and their maximum value. However, in the final part of the seismic motion the force $\boldsymbol{Q}_1$ computed with the full model shows a residual value equal to about 35% of the instantaneous maximum value. This residual force is caused by a permanent relative movement occurring between the foundations of the pier and the abutment. Of course, this result cannot be reproduced by the macro-element calculation, which does not model explicitly the pier foundations. However, the results of a parametric study on the stiffness and strength of simple structural configurations (omitted for the sake of brevity) showed that this permanent effect is significant only for bridges with a stiff structural response, like the one under examination that has a fundamental longitudinal period related to the axial stiffness of the deck.

Overall, the macro-element proved capable of reproducing with a reasonable accuracy the local seismic behaviour of a bridge abutment, with a significant gain in computational efficiency: the calculation time for the local model of abutment with a macro-element was about one order of magnitude smaller than the time needed to analyse the full model of Fig. 2.

APPLICATION TO A CASE STUDY

The macro-element presented in the above section was employed in the analysis of a multi-span girder bridge inspired by the Pantano viaduct (Gorini & Callisto, 2017; Gorini, 2019), designed as the approaching structure to the Messina Strait suspension bridge, in Italy (Brancaleoni *et al*., 2010; Callisto *et al*., 2013). From this case study, a simplified soil–bridge system was developed, reflecting the main mechanical properties of the Pantano subsoil and including an idealised representation of the structure; the reader can refer to Gorini (2019) for a detailed description of the numerical model. The reference model, depicted in Fig. 9, includes the bridge structure and the upper layers of the Messina gravels, extending down to a depth of 112 m from the foundation level. The full model, implemented in OpenSees, is composed of 268 703 elements for a whole plan extension of 262×72 m^2.

The bridge superstructure has a continuous deck supported by two central piers and by the lateral abutments. An alternating strong and weak contact is provided between the deck and the vertical elements, intended as a three-directional bearing device (rigid constraint) and a bi-directional device (longitudinal displacement allowed), respectively. In this way, the strong abutment carries most of the longitudinal inertial forces developing in the superstructure. The abutments are identical to that of the model in

Table 1. Parameters of the PDMY model adopted for the foundation soil and the embankment

Variable	Description	Foundation soil	Embankment
ρ: Mg/m^3	Mass density	2·243	2·039
G_r: kPa	Elastic shear modulus at p'_r	$9{\cdot}5 \times 10^4$	$1{\cdot}15 \times 10^5$
ν	Poisson ratio	0·2	0·2
p'_r: kPa	Reference mean pressure	80·0	80·0
d	Pressure dependence coefficient	0·5	0·5
$\gamma_{d,max}$	Peak shear strain	0·1	0·1
Φ_{PTL}	Phase transformation angle	26°	26°
c_1	Contraction parameters	0·045	0·013
c_2		5·0	5·0
d_1	Dilation parameters	0·06	0·3
d_2		3·0	3·0
M	Critical stress ratio	1·59	1·59
λ_c		0·02	0·02
e_0	Critical state line parameters	0·9	0·9
ξ		0·7	0·7
N	Number of yield surfaces	40	40

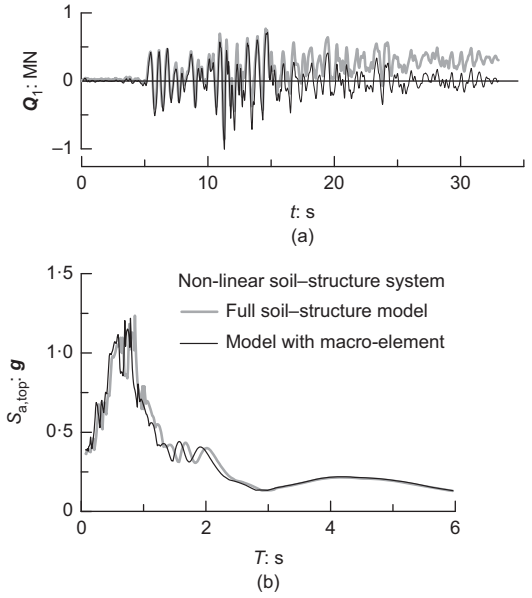

Fig. 8. Comparison between the results obtained with the fully non-linear soil–structure model and with the soil–abutment model with a bilinear macro-element: (a) time histories of the longitudinal interaction force; (b) 5%-damped elastic response spectra computed at the abutment top

Fig. 2. Because of their large strength, the structural members of the abutments were modelled through the ShellMITC4 elements (Dvorkin & Bathe, 1984) with an elastic behaviour, using constitutive parameters relative to a C32/40 strength class concrete in the European standards. The deck and the piers were modelled as beam elements with a visco-elastic behaviour. Energy dissipation was reproduced by assigning a Rayleigh damping of 2% to all the structural elements, calibrated on the significant vibration modes of the bridge.

The mechanical behaviour of the foundation soil was described assigning to the PDMY model the parameters reported in Table 2. The entire soil domain, assumed to be dry, was discretised through the SSPbrick eight-node hexahedral elements (Zienkiewicz & Shiomi, 1984). The embankment was reproduced as an equivalent single-phase body using the PDMY model to simulate its cyclic behaviour (Table 2). An additional small Rayleigh damping ratio was assigned to the soil elements to provide some dissipation at very low strain levels.

The soil–structure contact was modelled with thin solid elements interposed between the structure and the soil, with a friction angle equal to that of the soil as a reasonable assumption for soil–concrete contact.

After a first calculation stage aimed at reproducing the geostatic stress state, the abutment structure, the embankment and the bridge structure were built sequentially in the model. This static analysis was followed by the dynamic simulation, in which the use of parallel computing, obtained with the OpenSeesSP interpreter (McKenna & Fenves, 2008), was needed to obtain reasonable computation times. In the static stage, the displacements at the bottom of the grid were impeded in both directions, whereas only the horizontal displacements normal to each boundary were restrained along the lateral sides. In the subsequent dynamic phase, the restraints in the direction of motion were substituted with periodic constraints, imposing the same displacement to nodes located at the same elevation on opposite vertical boundaries. The longitudinal component of the Tabas record (Fig. 4) was considered and applied to the lower boundary of the model as a displacement–time history.

To reproduce the dynamic behaviour of the bridge structure, a uniaxial elastic macro-element was identified for the bridge in the longitudinal direction. Specifically, the transfer function was obtained by applying the procedure described in the previous section, and is shown in Fig. 10 with a continuous line. This function is characterised by a bimodal response and as for the case in Fig. 2 the dominant peak at $T = 0{\cdot}05$ s is associated with a combined global response, in which the higher modes of the vertical elements activate the dynamic axial response of the deck. The corresponding mass participation factor is equal to 10%, which corresponds approximately to the mass of the deck. A second peak with a lower amplitude occurs at $T = 0{\cdot}12$ s and is produced by the first global mode in the longitudinal direction: the strong pier bends according to a first mode shape, carrying a lower amount of the deck mass. In spite of the larger mass participation, equal to 55·4%, this mode produces a more limited effect in terms of inertial forces transferred to the abutment because the bending of the strong pier occurs at long periods and does not activate the dynamic response of the deck in its axial direction.

The transfer function in Fig. 10 was reproduced by a macro-element consisting of an equivalent 2DOF system calibrated on the peaks of the function $\boldsymbol{K}_{11}$ of the structure. As in the previous case of Fig. 2, the masses and the damping

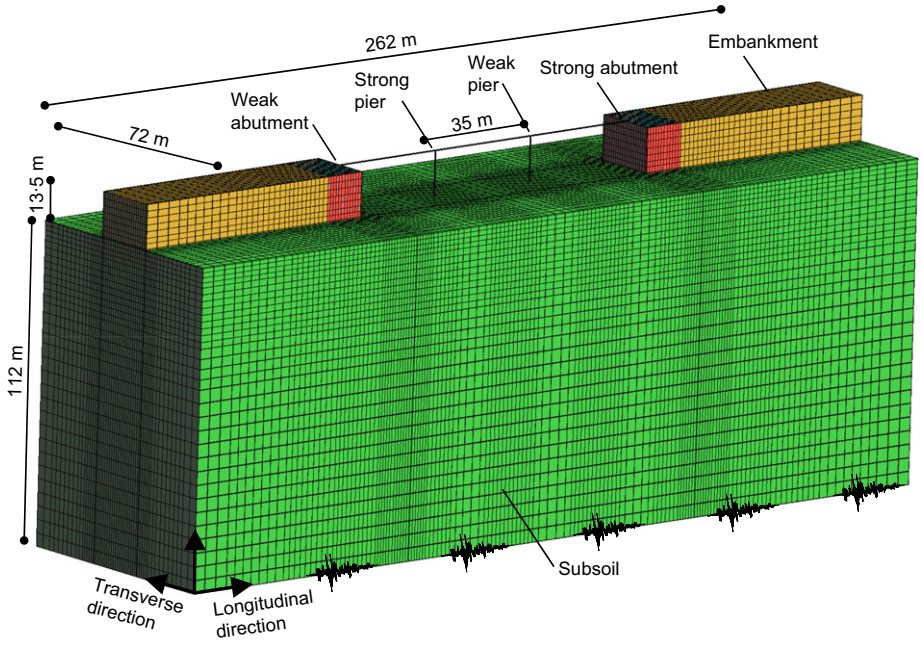

Fig. 9. Full model of the reference soil–bridge system implemented in OpenSees

Table 2. Parameters of the PDMY model assigned to the soil layers of the soil–bridge model

Variable	Messina gravels	Embankment
	$z > 30$ m/$z < 30$ m	
ρ: Mg/m^3	2·243/2·039	2·039
G_r: kPa	$1{\cdot}3 \times 10^5$	$1{\cdot}1 \times 10^5$
ν	0·2	0·2
p'_r: kPa	80·0	80·0
d	0·5	0·5
$\gamma_{d,max}$	0·1	0·1
Φ_{PTL}	17°	17°
c_1	0·195	0·195
c_2	0·0	0·0
d_1	0·6	0·6
d_2	3·0	3·0
M	1·59	1·42
λ_c	0·0219	0·0219
e_0	0·4478	0·4478
ξ	0·7	0·7
N	40	40

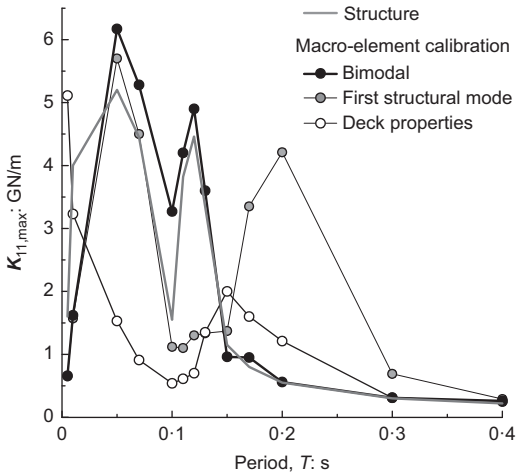

Fig. 10. Longitudinal transfer function $\boldsymbol{K}_{11}$ of the viaduct obtained with the full soil–bridge model and with the local soil–abutment model with macro-element

coefficients of the equivalent model reflect the modal characteristics of the structure, whereas the optimum values of the stiffness were found by trial and error. The resulting transfer function of the equivalent system is shown in Fig. 10 with full symbols, while Fig. 11 depicts the local finite-element model of the soil–abutment system in which the presence of the bridge structure is simulated with the macro-element.

In addition to the transfer curve of the proposed macro-element, Fig. 10 also shows the transfer functions obtained with different approaches to the calibration of the macro-element: (*a*) a calibration aimed to reproduce only the fundamental structural mode ($T = 0{\cdot}12$ s) (shaded symbols) and (*b*) a calibration based only on the deck properties (open symbols). The former solution (*a*) gives a transfer function that reproduces the dominant peak at $T = 0{\cdot}05$ s but moves the second peak to larger periods. Conversely, the calibration on the deck properties (*b*) alters completely the response of the system, producing the maximum amplitudes at very high frequencies ($T < 0{\cdot}005$ s).

Figure 12(a) compares the time histories of the longitudinal force at the deck–abutment contact $\boldsymbol{Q}_1$ obtained from the full model shown in Fig. 9 with the response of the local model that uses the macro-element to simulate the bridge structure (Fig. 11). Although the proposed macro-element is not capable of reproducing the residual value of $\boldsymbol{Q}_1$, it is seen to provide a good estimate of the maximum force transmitted to the abutment. In comparison, other options to represent the interaction of the abutment with the bridge structure, including that of not considering this interaction at all, yield very large errors.

The response spectra of the motion at the top of the abutment computed with the full model and with the proposed macro-element are very similar to each other, confirming that the proposed transfer functions are able to reproduce correctly the maximum amplitudes of the

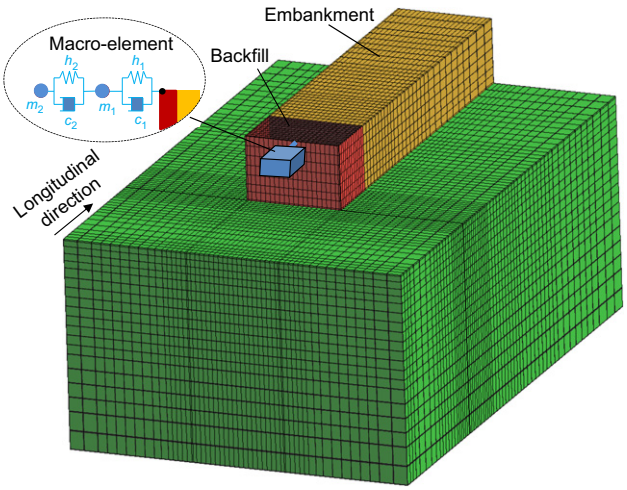

Fig. 11. Local soil–abutment model with an indication of the longitudinal macro-element

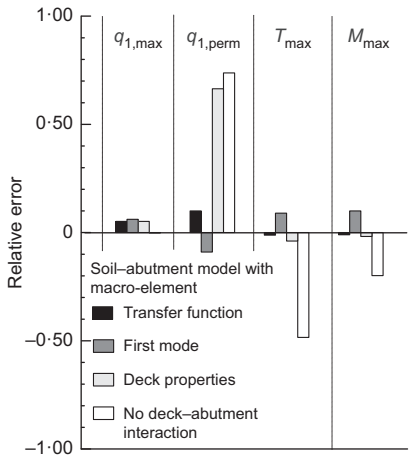

Fig. 13. Relative errors in displacements and internal forces in the abutment obtained with different descriptions of the dynamic response of the bridge structure

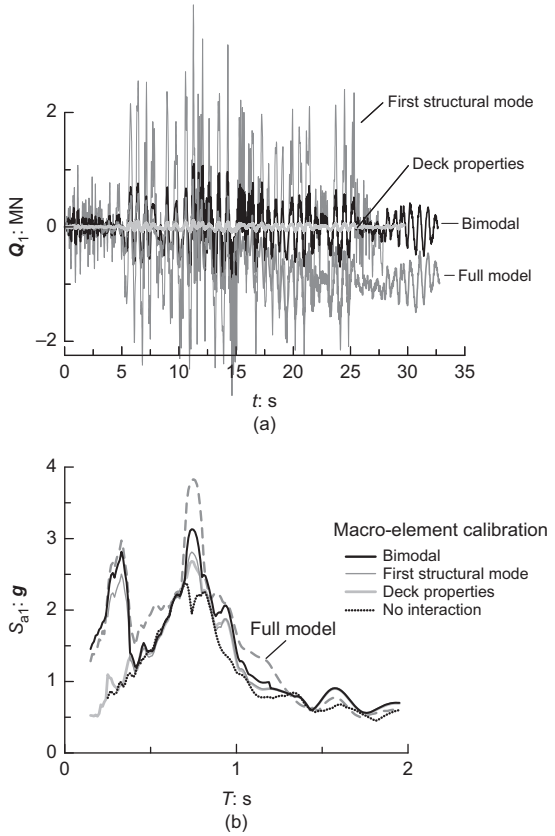

Fig. 12. Comparison between the response of the full and the local model: (a) time histories of the longitudinal interaction force Q_1; (b) 5%-damped elastic response spectra of the motion at the abutment top

earthquake-induced seismic motion and consequently the maximum interaction forces.

Figure 13 summarises the relative errors obtained in the prediction of the maximum and permanent displacements, $q_{1,max}$ and $q_{1,perm}$, of the abutment top and in the evaluation of the maximum internal forces at the base of the abutment wall, that is the maximum shear force T_{max} and bending moment M_{max}. The figure shows that the proposed macro-element is very good at predicting the maximum values of both the internal forces and the abutment displacement, while the permanent displacement of the top of the abutment is only slightly overestimated (by about 10% for the case at hand). Other options to calibrate the macro-element fail systematically to match both displacements and internal forces, with errors often in excess of 50%.

In order to highlight the practical importance of the present macro-element approach, it is worth mentioning that the computation time of the local model of the abutment with the macro-element was equal to 11 days, instead of the 90 days needed to analyse the full soil–bridge model, with a reduction of the computational demand of close to 90%.

CONCLUSIONS

In the current practice, it appears that there is no consensus on methods to account for the effects of soil–structure interaction on the seismic design of a bridge abutment. Given the difficulties in carrying out numerical analyses of large soil–structure interaction problems, and acknowledging the limitations of the decoupled approaches in reproducing the non-linearity of the behaviour shown by embedded foundations, it is tempting to take into account soil–structure interaction effects by introducing a partial soil–structure coupling in the analysis of the soil–foundation system. In this paper, this objective was pursued by developing a macro-element description of the bridge structure to represent efficiently in a local model of the bridge abutment the effect of the dynamic response of the bridge structure. The proposed methodology requires time-domain analyses, both for the calibration of the macro-element and for the analysis of the bridge abutment. Therefore, it may provide a useful analysis tool for the design of infrastructure of major importance, for which the costs associated with a design based on time-domain analyses is justifiable.

To date, the performance of the proposed model has been validated with reference to a limited number of cases and to the most important force components and degrees of freedom relevant for long girder bridges (longitudinal and vertical motion components). The applicability of the model for short bridges and for integral structural schemes needs further validation that is beyond the scope of the present paper.

The goal to reproduce with a compact model the dynamic response of a large bridge structure is quite ambitious, especially because a local soil–abutment model by definition cannot describe the interaction between the abutments and the pier foundations that occurs through the foundation soils.

This is the main reason why the proposed macro-element, in its present form, cannot reproduce the development of the permanent forces transmitted by the deck to the abutment. However, as design is often based on the maximum internal forces in the structure and on the maximum and residual displacements of the foundation elements, the proposed approach can be deemed appropriate for the seismic design of bridge abutments, as it provides a reasonable match with the results deriving from a full soil–structure interaction model.

NOTATION

$\boldsymbol{K}_{ij}$	transfer tensor of the macro-element
$k^{(1)}$	stiffness of the equivalent single-degree-of-freedom (SDOF) system
$k^{(\text{deck})}$	stiffness of the deck
$M_{\max}$	maximum bending moment at the base of the pier
$m^{(1)}$	mass of the equivalent SDOF system
$m^{(\text{deck})}$	mass of the deck
$\boldsymbol{Q}_{1,\text{ult}}$	ultimate limit value for the longitudinal interaction force $\boldsymbol{Q}_1$
$\boldsymbol{Q}_i$	interaction force exchanged at the deck–abutment contact in the i direction
$q_{1,\max}$	maximum instantaneous displacement of the abutment top in the longitudinal direction
$q_{1,\text{perm}}$	permanent displacement of the abutment top in the longitudinal direction
T	period
T_0	fundamental period of the soil deposit
$T_{\max}$	maximum shear force at the base of the pier
$\boldsymbol{u}_{1,\text{ult}}$	amplitude of the foundation displacement $\boldsymbol{u}_1$ associated with the attainment of $\boldsymbol{Q}_{1,\text{ult}}$
$\boldsymbol{u}_j$	input displacement of the abutment and pier foundations in the j direction
V_S	shear wave velocity of soil
ξ	damping ratio
$\xi^{(1)}$	damping ratio of the equivalent SDOF system

REFERENCES

Brancaleoni, F., Diana, G., Faccioli, E., Fiammenghi, G., Firth, I. P. T., Gimsing, N. J., Jamiolkowski, M., Sluszka, P., Solari, G., Valensise, G. & Vullo, E. (2010). *The Messina Strait bridge. A challenge and a dream*. Leiden, the Netherlands: CRC Press/Balkema.

Callisto, L. & Rampello, S. (2013). Capacity design of retaining structures and bridge abutments with deep foundations. *J. Geotech. Geoenviron. Engng ASCE* **139**, No. 7, 1086–1095.

Callisto, L., Rampello, S. & Viggiani, G. M. B. (2013). Soil-structure interaction for the seismic design of the Messina Strait bridge. *Soil Dyn. Earthq. Engng* **52**, 103–115.

Diaz, N. D. & Amat, P. S. (1999). *GID the personal pre/postprocessor user's manual, version 5.0*. Barcelona, Spain: CIMNE. See http://gid.cimne.upc.es (accessed 30/11/2019).

Dvorkin, E. N. & Bathe, K. J. (1984). A continuum mechanics based four node shell element for general nonlinear analysis. *Engng Comput. (Swansea)* **1**, March, 77–88.

Gorini, D. N. (2019). *Soil–structure interaction for bridge abutments: two complementary macro-elements*. PhD thesis, Sapienza University of Rome, Rome, Italy. See https://iris.uniroma1.it/handle/11573/1260972 (accessed 10/12/2019).

Gorini, D. N. & Callisto, L. (2017). Study of the dynamic soil–abutment–superstructure interaction for a bridge abutment. In *Proceedings of the 1st European conference on OpenSees (OpenSees days Europe 2017)* (eds H. Varum, J. M. Castro, L. Macedo, N. Pereira, X. Romao and G. Monti), pp. 57–60. Porto, Portugal: Faculty of Engineering, University of Porto.

Kausel, E. (2010). Early history of soil–structure interaction. *J. Soil. Dyn. Earthq. Engng* **30**, No. 9, 822–832.

McKenna, F. (1997). *Object-oriented finite element analysis: frameworks for analysis, algorithms and parallel computing*. PhD thesis, University of California, Berkeley, CA, USA.

McKenna, F. & Fenves, G. L. (2008). *Using the OpenSees interpreter on parallel computers*, NEESit, TN-2007-16, v1.0. Berkeley, CA, USA: University of California, Berkeley. See http://opensees.berkeley.edu/OpenSees/parallel/TNParallelProcessing.pdf (accessed 30/11/2019).

McKenna, F., Fenves, G. L., Scott, M. H. & Jeremic, B. (2000). *Open system for earthquake engineering simulation*. Berkeley, CA, USA: University of California, Berkeley. See http://opensees.berkeley.edu (accessed 30/11/2019).

Neuenhofer, A. & Filippou, F. C. (1997). Evaluation of nonlinear frame finite-element models. *J. Struct. Engng ASCE* **123**, No. 7, 958–966.

Neuenhofer, A. & Filippou, F. C. (1998). Geometrically nonlinear flexibility-based frame finite element. *J. Struct. Engng ASCE* **124**, No. 6, 704–711.

PEER (2019). *NGA-West2 – shallow crustal earthquakes in active tectonic regions. PEER ground motion database*. Berkeley, CA, USA: Pacific Earthquake Engineering Research Center, University of California. See https://ngawest2.berkeley.edu (accessed 30/11/2019).

Price, T. E. & Eberhard, M. O. (2005). Factors contributing to bridge-embankment interaction. *J. Struct. Engng ASCE* **131**, No. 9, 1345–1354.

Vamvatsikos, D. & Cornell, A. (2002). Incremental dynamic analysis. *Earthq. Engng Struct. Dyn.* **31**, No. 3, 491–514.

Yang, Z., Elgamal, A. & Parra, E. (2003). A computational model for liquefaction and associated shear deformation. *J. Geotech. Geoenviron. Engng ASCE* **129**, No. 12, 1119–1127.

Zienkiewicz, O. C. & Shiomi, T. (1984). Dynamic behavior of saturated porous media: the generalized Biot formulation and its numerical solution. *Int. J. Numer. Analyt. Methods Geomech.* **8**, No. 1, 71–96.